

Functional specificity and neural integration in the aesthetic appreciation of artworks with implied motion

Ionela Bara¹  | Kohinoor Monish Darda^{2,4}  | Andrew Solomon Kurz³  | Richard Ramsey⁴ 

¹Wales Institute for Cognitive Neuroscience, School of Psychology, Bangor University, Bangor, UK

²University of Glasgow, Glasgow, UK

³VISN 17 Center of Excellence for Research on Returning War Veterans, Central Texas Veterans Health Care System, Temple, Texas, USA

⁴Department of Psychology, Macquarie University, Sydney, Australia

Correspondence

Ionela Bara, Wales Institute for Cognitive Neuroscience, School of Psychology, Bangor University, Bangor LL57 2AS, United Kingdom.

Email: ionela.bara@bangor.ac.uk

Richard Ramsey, Department of Psychology, Macquarie University, Sydney 2109, Australia.

Email: richard.ramsey@mq.edu.au

Edited by: John Foxe

Abstract

Although there is growing interest in the neural foundations of aesthetic experience, it remains unclear how particular mental subsystems (e.g. perceptual, affective and cognitive) are involved in different types of aesthetic judgements. Here, we use fMRI to investigate the involvement of different neural networks during aesthetic judgements of visual artworks with implied motion cues. First, a behavioural experiment ($N = 45$) confirmed a preference for paintings with implied motion over static cues. Subsequently, in a preregistered fMRI experiment ($N = 27$), participants made aesthetic and motion judgements towards paintings representing human bodies in dynamic and static postures. Using functional region-of-interest and Bayesian multilevel modelling approaches, we provide no compelling evidence for unique sensitivity within or between neural systems associated with body perception, motion and affective processing during the aesthetic evaluation of paintings with implied motion. However, we show suggestive evidence that motion and body-selective systems may integrate signals via functional connections with a separate neural network in dorsal parietal cortex, which may act as a relay or integration site. Our findings clarify the roles of basic visual and affective brain circuitry in evaluating a central aesthetic feature—implied motion—while also pointing towards promising future research directions, which involve modelling aesthetic preferences as hierarchical interplay between visual and affective circuits and integration processes in frontoparietal cortex.

KEY WORDS

aesthetic judgement, body shape, fMRI, motion perception, reward circuit

Abbreviations: ACC, anterior cingulate cortex; AE, aesthetic evaluation; AntIns, anterior insula; EBA, extrastriate body area; fMRI, functional magnetic resonance imaging; fROI, functional region of interest; IM, implied motion; LOO, leave-one-out cross-validation; mOFC, medial orbitofrontal cortex; MT, middle temporal area; PPI, psychophysiological interaction; PSC, percent signal change.

This is an open access article under the terms of the Creative Commons Attribution License, which permits use, distribution and reproduction in any medium, provided the original work is properly cited.

© 2021 The Authors. *European Journal of Neuroscience* published by Federation of European Neuroscience Societies and John Wiley & Sons Ltd.

1 | INTRODUCTION

The ability to experience the aesthetic qualities of art represents a fundamental characteristic of human cognition. For millennia, questions concerning art and aesthetic

experiences have been debated (Bell, 1914; Collingwood, 1958; Danto, 1964; Else, 1938) and continue to drive real-life behaviour via attendance to museums, galleries and live performances. Neuroaesthetics research has identified the involvement of widespread brain networks spanning visual, motor, affective and cognitive information processing units during aesthetic judgements (Boccia et al., 2016; Brown et al., 2011; Cattaneo, 2019, 2020; Chatterjee, 2003; Chatterjee & Vartanian, 2016; Garcia-Prieto et al., 2016; Kirsch et al., 2016; Pearce et al., 2016). However, current understanding of how the brain constructs aesthetic experiences is in its infancy. For example, it remains unclear which types of mental subsystems (e.g. perceptual, affective and cognitive) are involved in different types of aesthetic appreciation, as well as how information is integrated across different subsystems to generate aesthetic judgements. The current project extends current understanding of aesthetic judgements by harnessing advances in human neuroimaging techniques that are more optimally designed to assess the division of labour between, as well as the integration across, distinct information processing units.

Neuroaesthetics research has focussed on deconstructing features of visual art, such as form, colour, symmetry, complexity, luminance and contrast (Bar & Neta, 2006; Bona et al., 2015; Graham et al., 2016; Hayn-Leichsenring et al., 2020; Igaya et al., 2021; Jacobsen et al., 2006; Jacobsen & Höfel, 2003; Nadal et al., 2010; Palmer & Schloss, 2010; Van Geert & Wagemans, 2019; Vartanian et al., 2013). Although many different visual features of art have been studied from a neuroscientific perspective, it is maybe surprising that implied motion has only received limited attention (Di Dio et al., 2016; Kim & Blake, 2007; Thakral et al., 2012).

Traditionally, artists have used different form and line cues, such as stroboscopic effects, broken symmetry or action lines to successfully evoke motion in static images (Cutting, 2002). Art theorists have supported the idea that motion cues in visual art might be particularly salient and engaging and therefore inextricably linked to aesthetic appreciation (Arnheim, 1950). In addition, Gombrich (1964) and (Wölfflin, 1942/2012) have pointed out that the discovery of motion cues in visual art shaped standards in art production and art perception and contributed to an art styles' definitional features. An illustration of typical implied motion cues used in visual art to is provided below (Figure 1).

Implied motion cues represent a useful target of study from a neuroscientific perspective because of the well-developed understanding of how sensitivity to implied motion is organised in the visual system. In non-human animals, as well as humans, observing moving visual

stimuli engages a brain region in posterior lateral occipitotemporal cortex, which is known as middle temporal area (MT) (Beauchamp et al., 2002; Maunsell & Van Essen, 1983; Zeki, 1974). Static images with implied motion cues are also able to create the illusory perception of motion while also engaging the same cortical region of MT (Kourtzi & Kanwisher, 2000; Lorteije et al., 2006; Osaka et al., 2010; Senior et al., 2000). Moreover, research has demonstrated that art images that imply dynamics tend to be judged as more aesthetically pleasing than static art images (Di Dio et al., 2016; Massaro et al., 2012; Mastandrea & Umiltà, 2016), which further reinforces the utility of implied motion cues as a model system to study.

Alongside motion cues, much of the history of art has been dedicated to the human figure (Berger, 1972; Clark, 1984), with the representation of a human figure in dynamic postures playing a central role in visual art expression (Adler & Pointon, 1993; Barasch, 1991; Flynn, 1998). Related human neuroscience research has shown that dedicated patches of occipitotemporal cortex and fusiform gyri respond more when individuals are shown images of bodies compared with non-body stimuli, such as houses or chairs (Downing & Peelen, 2011). The region in occipitotemporal cortex is known as extrastriate body area (EBA), due to its role in body-part processing.

Although implied motion cues appear well placed as a target of study in neuroaesthetics, only a few neuroscientific investigations of implied motion cues have been undertaken to date (Di Dio et al., 2016; Kim & Blake, 2007; Thakral et al., 2012). The findings so far regarding the role of brain area MT in aesthetic judgements have been mixed. Thakral et al. (2012) showed that motion-selective area MT was involved in processing implied motion cues but that it did not contribute to aesthetic appreciation of such cues. In contrast, Di Dio et al. (2016) found that a brain area in occipitotemporal cortex, which was presumed to be MT, was sensitive to the aesthetic judgements based on implied motion. Kim and Blake (2007) also showed that MT responded to aesthetic judgements based on implied motion cues, but only in a small number of participants (five per group) and only in those with prior art experience. Moreover, in the Kim and Blake (2007) study, motion cues and aesthetic preference covaried, such that it is impossible to disentangle the two influences on MT.

On balance, therefore, there is suggestive but mixed evidence for the claim that elementary visual processing units, such as MT, are involved in aesthetic appreciation of art. Indeed, the most comprehensive study to date in terms of sample size and the use of control conditions did not functionally define MT as a region of interest, which makes claims regarding functional specificity difficult

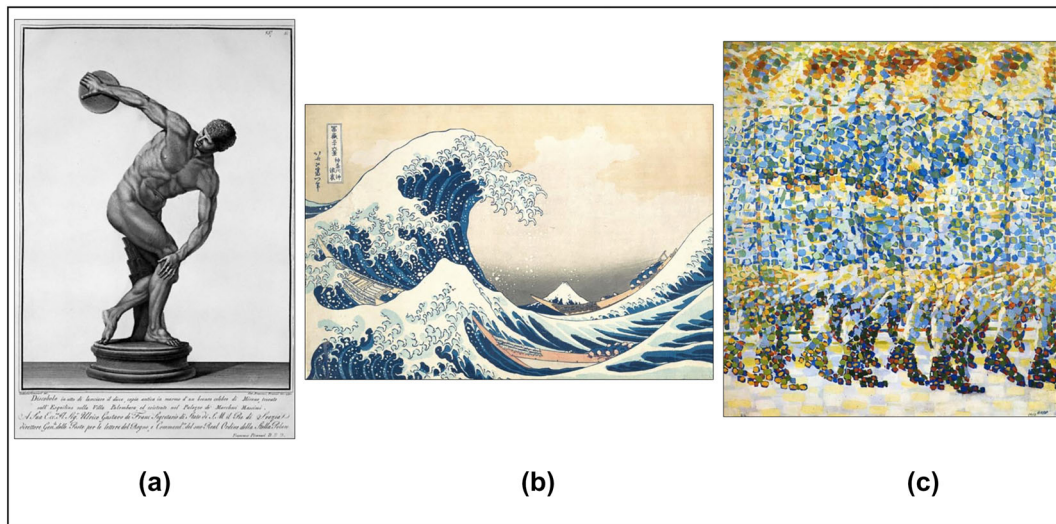


FIGURE 1 Examples of motion cues used in art. (a) Extreme contrapposto: *Discus Thrower* by Giovanni Battista Piranesi, 18th century. (b) Action lines: *The Great Wave off Kanagawa* by Katsushika Hokusai (1831). (c) Stroboscopic effects: *Girl running on a balcony* by Giacomo Balla (1912)

(Di Dio et al., 2016). Moreover, given recent concerns over questionable research practices and low levels of reproducibility in psychology and neuroscience (Button et al., 2013; Open Science Collaboration, 2015; Simmons et al., 2011), the current quality of evidence is only able to provide a weak foundation for a cumulative science of neuroaesthetics to develop. Therefore, it may be prudent for the field to develop a firm footing via more robust methodological approaches and embracing the credibility revolution (Ramsey, 2020; Vazire, 2018). Via the adoption of open science practices (e.g. preregistration and open data), as well as using more robust methods to estimate effect sizes across participants, one contribution of the current work, therefore, is to provide a more credible platform for future studies to build upon.

Although many visual features of art undoubtedly contribute to aesthetic preferences, the visual system alone cannot provide a complete understanding of the biological bases of how such judgements are constructed. Brain circuits associated with reward and pleasure are likely to be involved, because the experience of art has been described as pleasurable and gratifying (Dutton, 2009). In support of this view, human neuroscience experiments have shown that aesthetic judgements are linked to greater activation of brain networks associated with reward processing (Boccia et al., 2016; Brown et al., 2011; Di Dio & Vittorio, 2009; Kirsch et al., 2016). The reward brain network is known to be engaged in processing hedonic experiences and consists of the ventral striatum, interconnected with medial prefrontal and orbitofrontal cortex, the amygdala, anterior cingulate cortex and insular cortex (Berridge et al., 2009). What is

less clear currently is how signals from reward circuits and the visual systems are integrated during the construction of aesthetic judgements.

The current state of understanding in neuroaesthetics is limited by the modal method and approach used, which relies on fMRI and whole-brain mapping approaches. Whole-brain mapping approaches are useful to identify the involvement of large-scale networks, but they make it difficult to support strong claims about the functional regions identified in response to a task. Moreover, studies typically rely on ‘reverse inference’, whereby engagement of a given region is taken as evidence for a particular cognitive process (Poldrack, 2006). Such approaches suffer from poor functional specificity, and it is unclear to what extent specific functional regions are engaged by particular processes. For example, claims regarding the role of frontoparietal cortex in ‘mirroring’ processes, as well as a role for MT in sensitivity to motion and aesthetic preferences (Di Dio et al., 2016), could equally easily be explained by processing demands that are not specific to aesthetic evaluations such as attention.

For a deeper understanding of the links between the aesthetic experience and mental structure, steps are required that move beyond a reliance on reverse inference approaches. In the current work, we do so by demonstrating functional specialisation through a functional region-of-interest (fROI) approach. fROI approaches using novel analytical pipelines have been developed to standardise the approach to minimise subjectivity while optimising sensitivity (Julian et al., 2012; Nieto-Castañón & Fedorenko, 2012). fROI approaches,

therefore, are a powerful way to assess the division of labour in information processing by first identifying functional units and then testing how they respond during a task of interest, such as aesthetic judgements.

A further general limitation of the modal fMRI approach to studying aesthetic judgements has been the dominance of univariate methods. Univariate analyses measure the average activity across a set of contiguous voxels in a given brain region. Given the complexity of aesthetic judgements, there is a need, therefore, to move into multivariate space (Kriegeskorte, 2009; Norman et al., 2006). Some neuroaesthetics work has started to approach questions using multivariate classifiers (Iigaya et al., 2021). More generally, human neuroscience research on functional integration or how multiple brain systems interact with one another for a given process (Bullmore & Sporns, 2009; Park & Friston, 2013) is particularly relevant here because we want to estimate how and when signals from distinct circuits are integrated in the process of constructing an aesthetic judgement.

Across two experiments, we aim to provide a more comprehensive and fine-grained assessment of the cognitive and neurobiological architecture that underpins the aesthetic judgement of visual art. Specifically, we focus on aesthetic judgements of implied motion cues due to the long history of interest in motion cues in aesthetics generally, and the tractable properties that implied motion cues provide from a human neuroscience perspective. First, we use behavioural measures to investigate the various factors that impact aesthetic appreciation. Second, to gain a deeper insight into the functional organisation of brain circuits, we use fMRI techniques that are more optimally designed to study the division of labour between distinct component processors (functional segregation), as well as the integration of signals across component processors (functional integration). Our experimental design permits comparison of stimulus features (Dynamic > Static), as well as task conditions, whereby we compare aesthetic judgements with judgements of implied motion and a control task.

2 | EXPERIMENT 1

2.1 | Introduction

There were three main reasons for running a separate behavioural experiment prior to the fMRI experiment. First, we wanted to validate the stimuli that we would later use during scanning by confirming that aesthetic appreciation is affected by various factors, such as familiarity, perceived dynamism and how evocative the artworks are in conveying a meaning (Biederman &

Vessel, 2006; Cutting, 2002, 2003; Kemp & Cupchik, 2007; Leder et al., 2014; Mastandrea & Umiltà, 2016). Second, we wanted to be able select stimuli that would be most effective at achieving our research aims. Third, we wanted to include a wider set of stimuli and types of judgements than would be possible during scanning (due to time constraints) in order to more fully characterise the relationship between implied motion cues and perceptual inferences. More specifically, we wanted to address two questions in the behavioural experiment: (1) To what extent do implied motion cues impact judgements of artworks across a range of dimensions including aesthetic appreciation, perceived dynamism, familiarity and evocativeness? (2) To what extent do implied motion cues influence aesthetic judgements when accounting for other factors such as familiarity and evocativeness?

2.2 | Materials and methods

2.2.1 | Participants

Forty-five participants completed the behavioural experiment (31 females, $M_{age} = 20.73$ years, $SD_{age} = 4.83$). Participants received course credit or monetary compensation (£6). They gave informed consent before starting the experiment, and all procedures were approved by the Research Ethics and Governance Committee of the School of Psychology at Bangor University.

2.2.2 | Preregistration

We chose not to preregister the behavioural experiment because it primarily served to confirm our expectations based on prior work and provide a means to select stimuli for the fMRI component of the study. Therefore, it served a preparatory rather than confirmatory function. Consequently, we felt that the preregistration was more vital for the fMRI study than the behavioural study. For the fMRI component of the study (Experiment 2), we preregistered our primary research questions, analyses, data collection stopping rule and any exclusion criteria prior to embarking with data collection (<https://aspredicted.org/qr75g.pdf>).

We largely adhered to our preregistration commitments, with one notable exception, which we justify here. Our primary preregistered analytical approach involved the use of repeated measures ANOVA and subsequent paired comparisons. However, a well-documented weakness of such an approach is that it ignores the hierarchical or multilevel nature of the data (Barr et al., 2013). As

such, we chose to adopt a more complex modelling approach that could accommodate the multilevel structure of our data (Barr et al., 2013; Yarkoni, 2020). Importantly, we still test the same preregistered directional predictions, but we do so in a more comprehensive statistical manner. For completeness, we also calculate our preregistered analyses and make the results from all analyses available in supplementary materials, as well as online (see next section on open data and analyses). For both experiments, we use the same general analytical and modelling approach.

2.2.3 | Open data and analysis statement

In line with open science initiatives (Munafò et al., 2017), all the raw data for behavioural and fROI analyses are freely available on the Open Science Framework (<https://osf.io/x5d2g/>). We also include our analysis scripts that are associated with these analyses. We provide all the art stimuli used on both behavioural and fMRI experiments that are not protected by copyright. Finally, we include the whole-brain t-maps on NeuroVault.org. By providing the data online, we facilitate other researchers to pursue more exploratory analyses or examine alternative hypotheses.

2.2.4 | General analytical strategy

Wherever possible, we performed data analyses in the R programming language (R Core Team, 2020). Our general analysis strategy followed a Bayesian estimation approach to multilevel modelling (McElreath, 2020). The basic logic is to estimate parameters of interest in multilevel models and perform model comparison between simpler and more complex models. One advantage of a Bayesian estimation approach is that it naturally encourages consideration of uncertainty regarding inferences because the key result is the complete posterior distribution, rather than a point estimate (Kruschke & Liddell, 2018; McElreath, 2020).

More specifically, we followed a recent translation of McElreath's (2020) general principles into a different set of tools (Kurz, 2020). As such, we use the Bayesian modelling package 'brms' to run multilevel models (Bürkner, 2017, 2018). brms operates as front-end package for the Stan programming suite (Carpenter et al., 2017) and uses the same syntax as the popular 'lme4' package for estimating multilevel levels in a frequentist framework (Bates et al., 2015). Furthermore, our general data workflow follows the 'tidyverse' principles (Wickham & Grolemund, 2016), and we generate

plots using the associated data plotting package 'ggplot2', as well as the 'tidybayes' package (Kay, 2020).

2.2.5 | Stimuli

An initial stimuli database contained 80 images of representational paintings depicting either natural landscapes (40 images) or full human bodies (40 images). The images were characterised by a realistic pictorial style and were selected considering 19th- to 20th-century European and American art, as historical reference. These images were gathered from various websites, including WikiArt and Wikimedia Commons, and from web-based art galleries. Each category (landscape or human) was split further into static and dynamic by selecting stimuli with or without a clear sense of implied motion. Therefore, the stimuli fell into one of four different categories within a 2 (painting type: landscape or human) by 2 (dynamism: static vs. dynamic) factorial design.

2.2.6 | Task and procedure

The experimental rating task was produced in PsyToolkit (Stoet, 2010, 2017). The task involved participants rating 80 art images on four dimensions: familiarity, implied motion, aesthetic evaluation and evocativeness. All ratings were assessed on a 5-point Likert scale (1–5; *not at all* to *extremely*). On each trial, participants were presented with an art image, which remained on-screen until the participant made a rating response to all of the four questions using a computer mouse (Figure 2). Overall, the rating task had 80 trials. The trials were completely randomised, whereas the order of the questions within each trial was fixed. The experiment was performed in one laboratory-based session that lasted approximately 30 min.

2.2.7 | Data analysis

Given that the dependent variable (DV) is an ordered category (a 1–5 rating scale), we used ordinal regression. We ran two different types of ordinal regression model—one for each question of interest. First, we ran a multivariate model, which included all four DVs. This model addressed the extent to which experimental factors within our design influenced each DV. Second, we ran a univariate model, which focussed specifically on our primary DV of interest—aesthetic evaluation. The univariate model addressed the extent to which experimental factors within our design influenced aesthetic judgements



Please rate the following

Item	Not at all	Slightly	Neutral	Very	Extremely
How familiar is this painting?	<input type="radio"/>				
How dynamic is this painting?	<input type="radio"/>				
How much do you aesthetically appreciate this painting?	<input type="radio"/>				
How evocative (emotional) is this painting?	<input type="radio"/>				

Click this button to continue

FIGURE 2 Example of task trial in Experiment 1

while accounting for the impact of familiarity and evocativeness.

We consider the multivariate modelling first. We calculated four multivariate models, which built in complexity. Model 1 was an ‘intercepts only’ model, just so that we could compare subsequent models that included predictors of interest to a model without any predictors. Model 2 included the type of painting as a predictor (landscape vs. human). Model 3 additionally included the level of implied motion as a factor (static vs. dynamic). Model 4 was the full model, which additionally included the interaction between painting type and motion. Factors were coded according to a deviation coding style, where factors sum to zero and the intercept can then be interpreted as the grand mean and the main effects can be interpreted similarly to a conventional ANOVA (<http://talklab.psy.gla.ac.uk/tvw/catpred/>). As such, both painting type and motion were coded as -0.5 (landscape/static) and 0.5 (people/dynamic).

Following the ‘keep it maximal’ approach to multi-level modelling (Barr et al., 2013), we included the maximal number of varying effects (or ‘random’ effects in frequentist language) that the design permitted. As such, across models with predictors (Models 2–4), varying intercepts and effects of interest were estimated for participants, and a varying intercept was included for stimulus items. We also included covariation between the

four DVs and predictors, by including the $|a|$ term in the model syntax below.

We set priors using a weakly informative approach (Gelman, 2006). Weakly informative priors differ from uniform priors by placing a constrained distribution on expected results rather leaving all results to be equally likely (i.e. uniform). They also differ from specific informative priors, which are far more precisely specified, because we currently do not have sufficient knowledge to place more specific constraints on what we expect to find. We used the probit link in our cumulative models, which means our priors are specified in a standardised metric (z-scores). We placed priors for the thresholds (or intercepts) at zero with a normal distribution of 1.5. We also allowed thresholds within the model to vary by stimulus item. The fixed effects or predictors, as well as the standard deviations, were centred around zero with a normal distribution of 1. This means that we expect effects of interest (population effects) to be around zero more than we do 1 unit of standardised difference. Given that effects are relatively small in psychology, we felt that this was reasonable expectation. Also, by using weakly informative priors, we allow for the possibility of large effects, should they exist in the data (Gelman, 2006; Gelman et al., 2013; Gelman & Hill, 2007; Lemoine, 2019). Moreover, a further advantage of weakly informative priors is that we would not expect the choice

of prior, as long as it remained only weakly informative, to matter too much because the data would dominate the structure of the posterior distribution.

The brms formula for multivariate model 4 is specified here:

```
brm (mvbind (familiarity,dynamism,aesthetic,evocativeness)
| thres(4,gr = item)
~ 1 + type * motion +
(1 + type * motion | a | participant) +
(1 | item) family = cumulative("probit"))
```

Given that aesthetic judgements specifically were our primary focus, we also ran a univariate model that only modelled aesthetic responses. Univariate models 1–4 had the same factorial structure as the multivariate models, as well as the same maximal varying effects structure. Model 5 additionally included familiarity ratings as a covariate in the design. Model 6 additionally included evocativeness ratings as a covariate in the design. Models 5 and 6, therefore, included predictors that were ordinal in structure. As such, we included familiarity and evocativeness as monotonic effects (Bürkner & Charpentier, 2020). We used the same priors as the multivariate model with the addition of monotonic priors for the two monotonic predictors. The size and direction of monotonic priors were specified as a normal distribution (0, 0.2), and the shape of the distribution across adjacent categories was specified in a uniform manner, as we had no particular prior expectations (Dirichlet[2,2,2,2]).

Univariate model 6 is specified here:

```
brm (aesthetic | thres(4,gr = item)
~ 1 + mo (familiarity) + mo (evocativeness) + type * motion +
(1 + mo (familiarity) + mo (evocativeness)
+ type * motion | participant( +
(1 | item) family = cumulative("probit")).
```

We interpreted the output of both model types using two main approaches. First, whenever possible, we performed model comparison via efficient approximate leave-one-out cross-validation (LOO; Vehtari et al., 2017). LOO is a way of estimating how accurately the model can predict out-of-sample data. Therefore, we took all models within a particular model type (multivariate or univariate) and asked how accurate they were at predicting the out-of-sample data. By doing so, we can

estimate how much increasing model complexity increases model accuracy. In cases where the efficient use of LOO was not possible, we used k-fold cross-validation, which is computationally more demanding and thus time consuming. Second, we also interpret the posterior distribution of our key parameters of interest within our factorial design. By combining model comparison with an evaluation of parameter estimates, we are able to make a judgement on how much additional variables add explanatory value to the model, as well as estimate the size and precision of our key effects of interest within our factorial designs, such as the effect of implied motion.

2.3 | Results

Rating data for all four DVs are visualised as a function of our primary conditions of interest (Figure 3). The overall familiarity ratings were low (between 1 and 2 points, on average), as illustrated in the upper panel of Figure 3. In addition, the artworks with implied motion cues conveyed greater dynamism were rated more aesthetically pleasing and more evocative than their static counterparts.

2.3.1 | Multivariate model results

The multivariate models appeared to mix well across different chains, and the model diagnostics were not concerning, which provides some guide that the models were functioning in a sensible manner. The same was true for all of the models across the two experiments. The chains, R-Hat, and Neff/N values for the full model in each analysis are available on our Open Science Framework page (<https://osf.io/x5d2g/>).

If we look at the model comparison values (Figure 4a), we can see that as expected all models with predictors performed better than the intercepts-only model (Model 1). We can also see that the error bars overlap across Model 3 and Model 4, indicating that they perform similarly. In addition, Model 3 and Model 4 perform better than Model 2, which only includes the type of painting (landscape vs. human). Therefore, we can conclude that adding implied motion as a factor improves the accuracy of the model (Model 3) but adding the interaction between painting type and motion (Model 4) does not.

Furthermore, when interpreting the parameter estimates of interest, we focus on the most complex model (Model 4). Illustrated in Figure 4b are the population (or ‘fixed’) effects from the full model across all four DVs

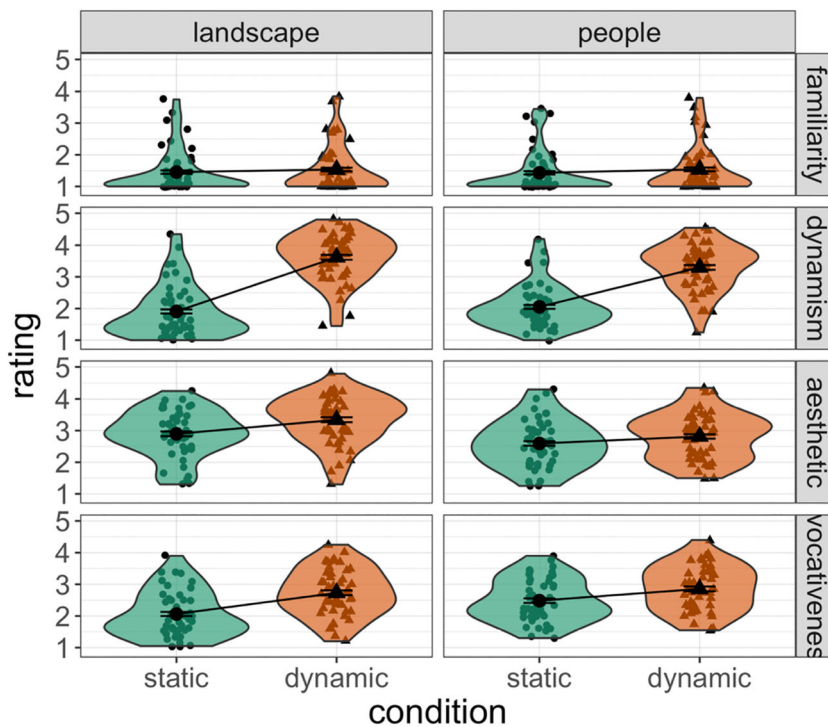


FIGURE 3 Experiment 1—rating judgements by question type and stimulus features. Ratings are reported on 5-point Likert scale (1–5; *not at all* to *extremely*). The upper panel shows the ratings for familiarity. The middle and lower panels show ratings for dynamism, aesthetic evaluation and evocativeness on static and dynamic conditions for artworks describing both landscape and people. The error bars represent 95% confidence intervals

(Table 1). Negative values are a bias towards landscapes or static images, whereas positive values are a bias towards paintings with people or implied motion. Regarding our key factor—the effect of implied motion across all four DVs—we can see a bias in ratings for dynamic stimuli in the predicted direction (Figure 4b). Indeed, the effect of implied motion is largest for motion ratings and smallest for familiarity ratings, whereas aesthetic and evocativeness ratings are in between these two posts. Therefore, in consensus with our hypotheses and previous work, these results confirm that the effect of implied dynamism is largest for motion judgements but is also present for evocativeness and aesthetic judgements. To complement the population or ‘fixed’ effects, in Supplementary Figure S1, we also visualise estimates of the varying parameters in the model. As such, we visualise the extent to which intercepts vary across items as well as how much the intercepts and population effects vary across participants. In addition, in Supplementary Figure S2, we plot the fixed effects from the model in the rating scale units so that the results can be viewed in the natural metric of points on a scale, as well as the model parameter units.

2.3.2 | Univariate model results

If we look at the model comparison values (Figure 5a), we can see that all models with predictors performed

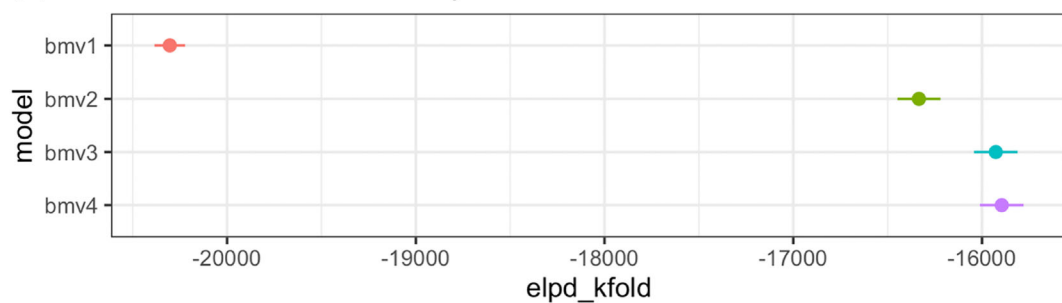
better than the intercepts-only model (Model 1). We can also see that Models 2–5 perform largely equivalently (in that error bars overlap) with only small differences between them. Model 6, which is the most complex model that includes covariates of familiarity and evocativeness performs better than the other models. Therefore, we can conclude that adding evocativeness ratings improves the accuracy of the model.

We now turn to interpret our key parameter estimate, which is the effect of implied motion. To do so, we display the parameter estimates across all models with predictors (Models 2–6; Figure 5b). We can see that the posterior distribution for the effect of implied motion is in the expected direction and does not overlap with zero in Models 3–5. In Model 6, the posterior distribution is partly overlapping with zero, but the majority of the distribution is supporting an aesthetic preference for dynamic over static images. Therefore, implied motion cues influenced aesthetic evaluations in the manner that we expected, even when including possible contributions of evocativeness and familiarity.

2.4 | Discussion

Experiment 1 demonstrated that implied motion cues in visual artworks influence aesthetic preferences in the manner that we anticipated, such that motion cues are perceived as more aesthetically pleasing than static

(a) Multivariate model comparison via kfold



(b) Multivariate model coefficient plot for fixed effects (predictors)

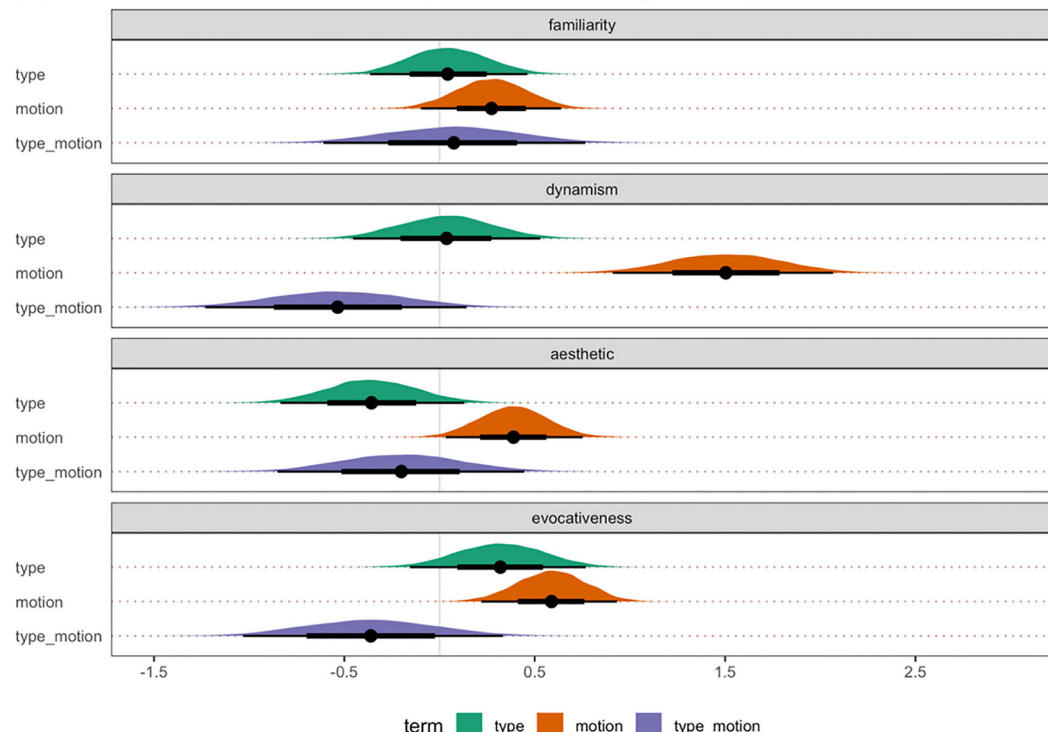


FIGURE 4 Experiment 1—multivariate model results. (a) Multivariate model comparison across Models 1–4. (b) Multivariate parameter estimates for the full model (Model 4) across all four dependent variables. Panel (a) illustrates the multivariate model comparison—all models performed better than the intercepts-only model. The structure of the multivariate models comprises Model 1, intercepts only; Model 2 includes painting type (landscape vs. human) as a predictor; Model 3 additionally includes motion type (static vs. dynamic) as a predictor; model 4 includes all predictors of interest, plus an interaction term between painting type and motion type. Panel (b) shows the multivariate parameter estimates for fixed effects in the full model across all four dependent variables: familiarity, dynamism, aesthetic appreciation and evocativeness. Note: In (a), $\text{elpd}_{\text{kfold}}$ = expected log pointwise predictive density; kfold = kfold cross-validation; Error bars = standard error of the mean; in (b), type = type of painting (landscape vs. human); motion = level of implied motion (static vs. dynamic); type_motion = interaction between type of painting and level of implied motion; Point estimate = median; Error bars represent 66% quantile intervals (thick black lines) and 95% quantile intervals (thin black lines)

paintings. Further, the effect of implied motion on aesthetic preferences could not be completely accounted for by familiarity or evocativeness ratings. Therefore, these results provided confidence that the chosen stimuli influence aesthetic preference in the manner that would be useful to address our neuroscientific questions in Experiment 2.

3 | EXPERIMENT 2

3.1 | Introduction

Experiment 2 aimed to provide deeper insight into the functional role of distributed but connected brain regions in the aesthetic processing of implied motion cues in

TABLE 1 Experiment 1—multivariate model fixed effects

DV	Term	Value	Lower	Upper
Familiarity	type	0.04	-0.37	0.46
	motion	0.27	-0.10	0.64
	type_motion	0.07	-0.61	0.77
Dynamism	type	0.04	-0.46	0.53
	motion	1.50	0.91	2.07
	type_motion	-0.54	-1.23	0.14
Aesthetic	type	-0.36	-0.84	0.13
	motion	0.39	0.03	0.75
	type_motion	-0.20	-0.85	0.45
Evocativeness	type	0.32	-0.16	0.77
	motion	0.59	0.22	0.93
	type_motion	-0.36	-1.03	0.33

Note: Labels for dependent variables and terms are similar to Figure 4. Point estimates and error bars are expressed as median and median absolute deviation.

visual art. We used fMRI to investigate the extent to which perceptual brain regions (EBA, MT) and affective reward brain regions are involved in aesthetic evaluation task, implied motion judgments and a control task. In addition, using a functional connectivity approach, we examined the extent to which visual seed regions (EBA, MT) are functionally coupled to regions in the affective (reward) network across aesthetic evaluation, implied motion and control tasks. We predicted that EBA and MT would show higher sensitivity to implied motion cues when evaluating aesthetics and implied motion. We also predicted that there would be more functional coupling between perceptual regions (EBA and MT) and the affective neural network for the aesthetic than implied motion evaluations.

3.2 | Materials and methods

3.2.1 | Participants

Twenty-seven participants ($M_{\text{age}} = 22.67$ years, $SD_{\text{age}} = 1.62$; 17 females) took part in the fMRI study. None of the participants took part in Experiment 1. All participants had normal or normal to corrected to normal vision and received a monetary compensation (£15). They gave informed consent before starting the experiment. Four participants were excluded due to excessive movement (>4 mm) during fMRI scanning. The final sample consisted of 23 participants (14 females, $M_{\text{age}} = 22.52$ years, $SD_{\text{age}} = 1.60$). All procedures were approved by the

Research Ethics and Governance Committee of the School of Psychology at Bangor University.

3.2.2 | Stimuli

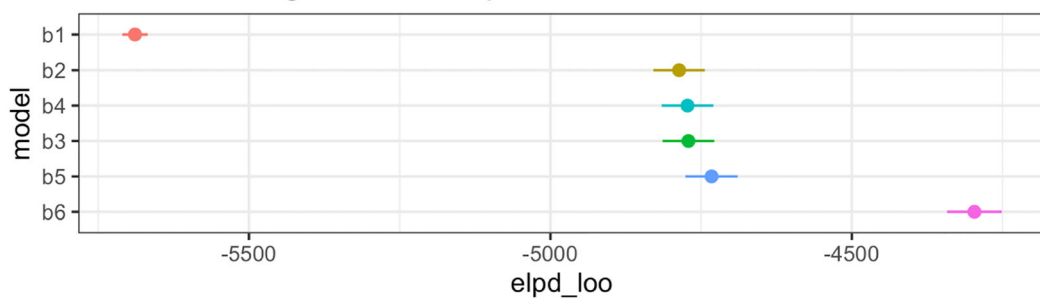
Due to time constraints during scanning, we chose not to include landscape and portrait stimuli together. As such, we chose to simplify the design by only focusing on stimuli depicting humans. Our overarching research question on the impact of dynamism on aesthetic preference could have been answered using landscapes or portrait stimuli, but because our laboratory has more experience studying social cognition and specifically body perception (e.g. Ramsey, 2018), we chose to focus on human stimuli. We selected 30 paintings from a total of 40 human images. The stimuli used in this fMRI study consisted of 30 images of representational paintings depicting one or more human forms. The bodies could be displaying two posture types: dynamic postures (15 images) and static postures (15 images). The images described humans in either outdoor or indoor scenes. The number of full body figures present in the images was balanced between two human bodies (14 images) and three or more human bodies (16 images). Each image was 785×774 pixels in size. For a comprehensive description of the stimuli used in this fMRI study, including the list of artworks, artists, year of production, and museum collection, see Supplementary Tables S1 and S2. Copyright permitting, all the images that we used are also available on our Open Science Framework page (<https://osf.io/x5d2g/>).

All visual stimuli were presented using MATLAB and PsychToolbox (Brainard, 1997; Pelli, 1997) and were projected on a computer screen mounted behind the magnet and observed through a mirror connected to the MR head coil.

3.2.3 | Design

This study used a repeated measures factorial design. There were two independent variables: stimuli type (two levels: dynamic and static) and task (three levels: aesthetic evaluation, implied motion and control). The dependent variable was the blood-oxygen-level-dependent (BOLD) haemodynamic response in functional regions of interest. Using this design ensured that we could investigate the extent to which separate functional networks contribute to aesthetic evaluation of artworks with implied motion.

(a) Aesthetic ratings model comparison via Loo



(b) Aesthetic model coefficient plot for fixed effects (predictors)

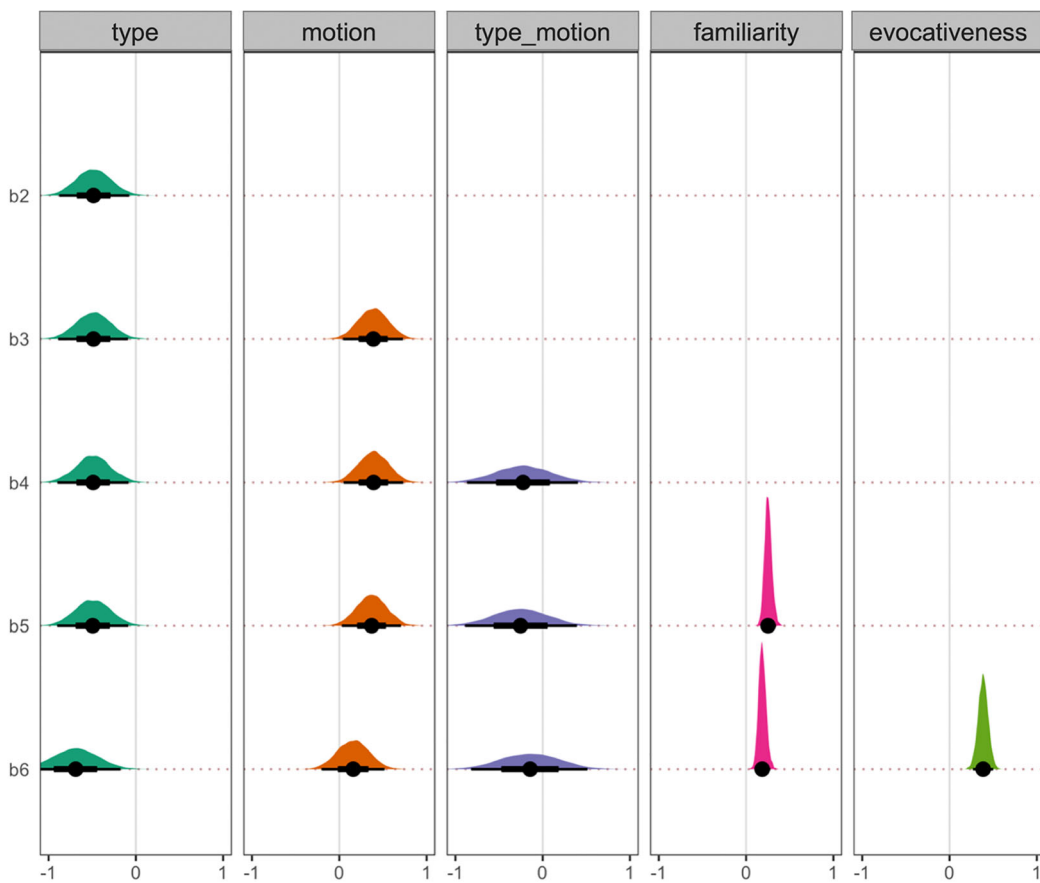


FIGURE 5 Experiment 1—univariate (aesthetics-only) model comparison. (a) Univariate model comparison (Models 1–6) on aesthetic judgements. (b) Univariate parameter estimates across Models 2–6, which contain predictors. Panel (a) illustrates model comparison performance on aesthetic judgement data—all models performed better than the intercept only model. Models 1–4 had an identical structure as the multivariate models. Model 5 - additionally including familiarity ratings as a covariate; model 6 - additionally includes evocativeness ratings as a covariate. Panel (b) shows parameter estimates for fixed effects across univariate (aesthetics) Models 2–6. Note: In (a), elpd_loo = estimate of the expected log pointwise predictive density; loo = leave-one-out estimated cross-validation; Error bars = standard error of the mean; in (b), type = type of painting (landscape vs. human); motion = level of implied motion (static vs. dynamic); type_motion = interaction between type of painting and level of implied motion; familiarity = familiarity as monotonic predictor; evocativeness = evocativeness as monotonic predictor; Point estimate = median; Error bars represent 66% quantile intervals (thick black lines) and 95% quantile intervals (thin black lines)

3.2.4 | Procedure

The study consisted of one session inside the MRI scanner. All participants completed the MT motion localiser task and the reward circuit localiser task. We already had EBA localiser data from a previous fMRI experiment for 15 of the participants, which means only eight participants completed the body localiser task as part of this project. Participants also completed the main experimental task, which was split into three separate scanning runs, with each run having a different task condition. The three main experimental task conditions were aesthetic evaluation, implied motion and a control task. The order of the tasks was counterbalanced so that each participant started with one of the localiser tasks, interspersed with the three main experimental tasks. For example, of 23 participants (including the eight participants for whom we already had the EBA localiser), 13 participants started with the MT motion localiser task, whereas 10 participants first completed the reward circuit localiser. The MRI scanning session lasted no more than 1 h. For exploratory purposes, at the end of scanning session, participants completed a pen on paper questionnaire to assess their general interest and expertise in art (Chatterjee et al., 2010). The results are reported in Supplementary Table S11.

3.2.5 | Functional localisers

MT motion Localiser

To localise motion-selective brain regions (MT), we used an established task developed by Jiang et al. (2015). The motion localiser consisted of alternating blocks of moving dots, stationary dots and fixation. The task comprised two runs, with each run including 30 10-s blocks. As the localiser task involved a passive observation, the order of the conditions was fixed: motion, static and fixation.

The visual stimuli were displayed within a circular shape (radius 8°) with a fixation cross in a central position. In the motion condition, the dots' speed was of 8° per second. All presented dots were white on a black background. Throughout the tasks, the participants were instructed to fixate at the centre of the screen and passively observe the visual stimuli. An illustration is provided below (Figure 6a).

EBA Localiser

To localise body-selective brain regions, we used an established localiser paradigm (Downing et al., 2007). The body localiser involves presenting separate 18-s blocks of human bodies (without heads), chairs, faces and scenes while using 40 different colour images per

category (size: 400 × 400 pixels). There were 24 trials per block, each trial duration of 750 msec. At presentation, each stimulus's position was jittered at 2° from central fixation cross. During each block, one stimulus was repeated twice, and participants were asked to respond by pressing a button whenever they noticed the same stimulus repeated (1-back task). An illustration is provided below (Figure 6b).

Reward network localiser

To define reward-selective brain areas, we created a block design task that used four different types of stimuli: positive-valence faces, neutral-valence faces, positive-valence objects and neutral-valence objects. All stimuli were previously validated in terms of positive and neutral valence and were retrieved from established databases (for faces: DeBruine & Jones, 2017; for objects: Blechert et al., 2019). All stimuli were equal in size (600 × 450 pixels) presented in a randomised order on a white background. The localiser consisted of 18-s blocks of 24 trials of positive faces, neutral faces, positive objects and neutral objects using 40 different colour images per category. At presentation, each stimulus's position was jittered at 2° from the central fixation cross. As in EBA body localiser task, participants had to indicate by pressing a button whether the same stimulus was repeated twice (1-back task). All participants were tested on two runs of this reward localiser task. An illustration is provided below (Figure 6c).

3.2.6 | Main experimental tasks

The main experimental tasks consisted of three conditions: aesthetic evaluation (AE), implied motion (IM) and control. Although not common in neuroaesthetics research, we introduced a control task to enable a point of comparison to our experimental tasks and to help distinguish between the effects of aesthetic judgement and motion judgement at a behavioural and brain level. As previously demonstrated, a comparison between control measurements and the other experimental measurements increases the reliability of the results (Kirk, 2014). All participants performed one run of each experimental task. The order of the tasks was counterbalanced to avoid performance bias on either of the tasks. Of 23 participants, eight participants started with the AE task, eight participants started with the IM task, and seven participants started with the control task. For each task, 30 art stimuli (15 dynamic and 15 static) were presented in an event-related design, with a variable interstimulus interval (ISI) of 4–6 s. The same art stimuli were used for all three experimental tasks and were presented randomly

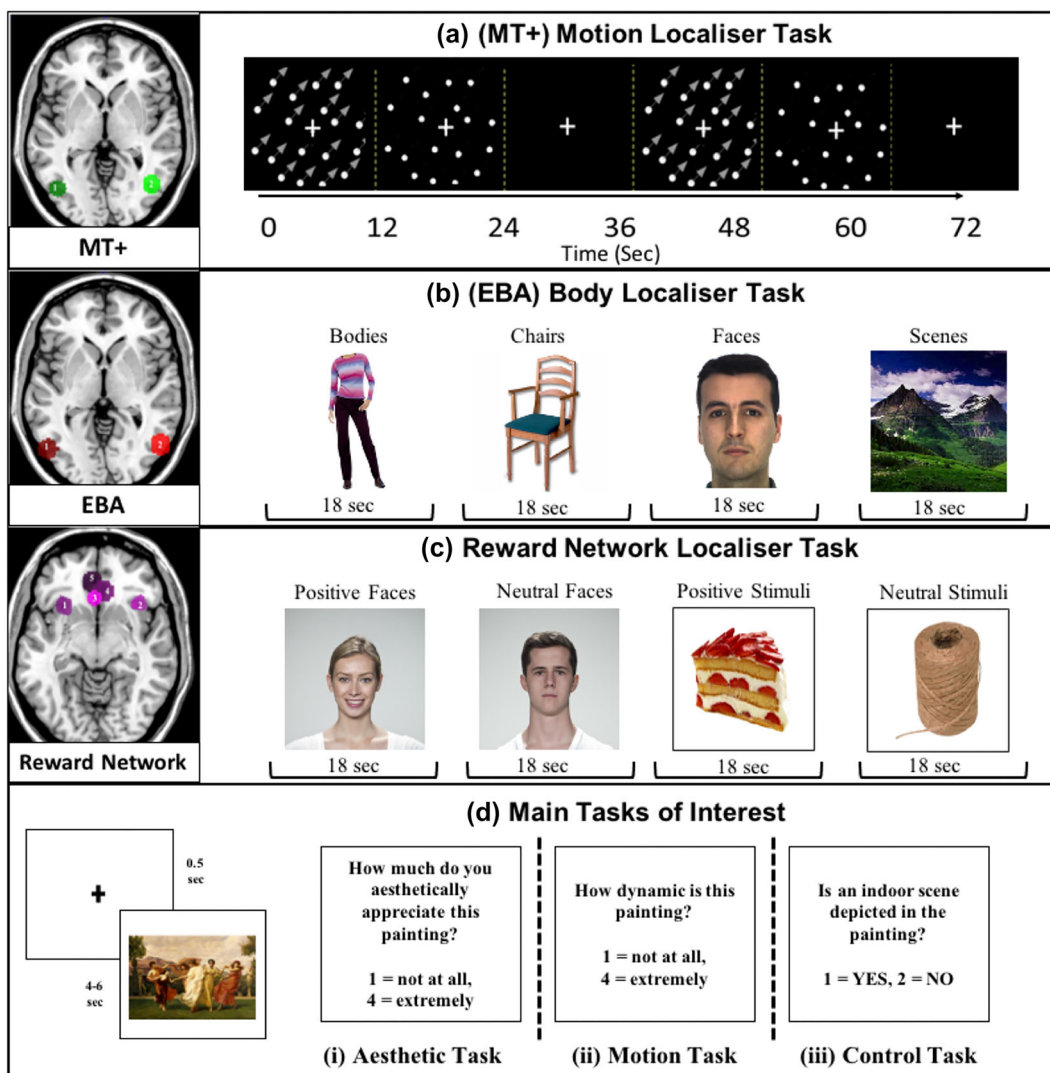


FIGURE 6 Stimuli for the functional localisers and main experimental tasks. Stimuli and trial design for the motion localiser task (a), the body localiser task (b), the reward network localiser task (c) and the main experimental tasks (d): aesthetic judgement task (i), implied motion task (ii), control task (iii)

for each participant; no stimulus was repeated on the same task. Following a central fixation cross, each image (785×774 pixels) was displayed on the middle of a white background. One functional run consisted of 30 trials, with a single run per task.

In the AE task, participants were instructed to make judgements about how much they aesthetically appreciate the paintings, whereas in the IM task, participants were asked to make judgements about the perceived level of implied motion on the paintings. On AE and IM tasks, the button pressing responses were recorded on a scale ranging from 1 to 4 (1 = *not at all*, 4 = *extremely*). On the control task, participants had to make a binary response (1 = *yes*, 2 = *no*) on the perceptual features of the painting, for example, ‘Is an indoor scene depicted in the painting?’ The questions’ text style had the following features: Calibri font, size 30, colour

black. A graphical representation of the main task is illustrated in Figure 6c.

3.2.7 | Data acquisition

Data were collected using a 3-T Philips Achieva full-body MRI scanner equipped with a SENSE phased-array 32-channel head coil. In order to attenuate the scanner noise, all participants were provided with earplugs and headphones. The participants were instructed to avoid head motion during scanning. The tasks’ responses were recorded using a four-button pressing box. Functional images were obtained using a T2*-weighted single-shot echo planar image sequence with the following functional task parameters: acquisition time (TR) = 2000 ms, echo time (TE) = 30 ms, flip angle = 90°, number of

axial slices = 35; slice thickness = 4 mm; slice gap = 0.8 mm; field of view = $230 \times 230 \times 167$ mm³.

Four dummy scans acquired at the beginning of each run of the task were not included in the analyses. A high-resolution T1-weighted anatomical image was also collected with the following parameters: repetition time = 12 msec, echo time = 3.5 msec, flip angle = 8°, number of axial slices = 170, voxel size = 1 mm³, field of view = $250 \times 250 \times 170$ mm³.

3.2.8 | Behavioural data analysis

We used the same approach as Experiment 1 with the following exceptions. First, we only had two DVs—motion and aesthetic judgements. Second, the design was simpler because we only had human bodies (there were no landscape paintings presented). Consequently, there were only two models—an intercepts-only model (Model 1) and a full model including the stimulus factor motion/dynamism (Model 2). Model 2 is displayed below:

```
brm (mvbind (dynamism, aesthetic) | thres(3, gr = item) ~ 1 + motion +
  (1 + motion|a|participant) +
  (1|item) family = cumulative("probit"))
```

3.2.9 | MRI data preprocessing and analyses

fMRI data were preprocessed and analysed using Statistical Parametric Mapping software (SPM8; Wellcome Trust Department of Cognitive Neurology, London, UK: www.fil.ion.ucl.ac.uk/spm/). Functional image preprocessing steps included correction for slice timing, re-alignment, co-registration, segmentation, normalization to the Montreal Neurological Institute (MNI) template with a resolution of 3 mm and spatially smoothing using 8-mm FWHM Gaussian kernel. Head motion was investigated for each functional run, and data were not analysed if head motion exceeded 4 mm in any direction.

For the localiser tasks, a design matrix was fit for each participant and consisted of regressors for each condition: dynamic and static for the MT motion localiser; bodies, chairs, faces and scenes for the EBA body localiser; and positive faces, neutral faces, positive objects and neutral objects for the reward network localiser. The onset and duration of each condition was defined and convolved with the standard hemodynamic response function. Contrast images were then calculated for each subject in order to identify regions that responded to motion (dynamic > static), bodies (bodies > other categories) and reward [positive (positive faces + positive objects) > neutral (neutral faces + neutral objects)].

For the main experimental tasks (AE, IM, control), a design matrix was fit for each participant with two regressors: one for dynamic stimuli and one for static stimuli. The onset and duration of each task was defined and convolved with the standard hemodynamic response function. Thus, for all three tasks separately, a Dynamic > Static contrast was calculated in order to identify regions of the brain that respond more to dynamic stimuli compared to static stimuli when making aesthetic and implied motion judgements, as well as when performing the control task.

In order to investigate the response profile of MT, EBA and the reward network, the group-constrained subject-specific (GSS) analysis pipeline was used (Fedorenko et al., 2010; Julian et al., 2012). Using the GSS approach has certain advantages over standard region-of-interest and whole-brain approaches because it decreases the amount of subjectivity that contributes to selecting individual fROIs and enhances functional resolution (Julian et al., 2012). The GSS analyses were implemented using the spm_ss toolbox via SPM (web.mit.edu/evelina9/www/funcloc.html).

According to the GSS procedure, functional ROIs for each participant were defined. These fROIs were determined considering firstly each subject's activation map for the localiser tasks and secondly group constraints or masks. These masks describe a group of parcels that delimit brain regions where prior independent research demonstrated to exhibit activity for the localiser contrasts. For each participant, these masks were used to constrain the selection of subject-specific functional ROIs. Based on t-values, the top 10% of the activated voxels within each parcel were selected as that individual's fROI. By using the top 10% of voxels instead of a fixed threshold, a constant size of each fROI is maintained across participants (Blank et al., 2014). A graphical illustration of the MT, EBA and reward network fROIs is presented in Figure 6. MT has been known to be sensitive to visual moving stimuli (Huk et al., 2002). Two parcels (left and right MT) were derived from group average MNI coordinates across several independent studies (Downing et al., 2007; Lewis et al., 2000; Peelen et al., 2006). For the MT masks, the dynamic > static contrast was used.

The EBA parcels were derived from group average MNI coordinates across several research studies (Downing et al., 2001; Downing et al., 2007; Lamm & Decety, 2008). Overall, these studies indicated a greater response in EBA to whole human body than to other object categories. Due to the fact that previous research suggested a strong right-hemisphere functional lateralization for the extrastriate visual areas (Willems et al., 2010), the results are reported for right EBA only. For the right EBA mask, the bodies > other categories contrast was used.

Regarding the reward localiser task, as we were only interested in those brain regions that have consistently shown involvement in aesthetic appreciation tasks, we selected the following parcels of the reward network: left anterior insula (L AntIns), right anterior insula (R AntIns), medial orbitofrontal cortex (Med OFC), right anterior cingulate cortex (R ACC) and left anterior cingulate cortex (L ACC). These parcels were derived from group average MNI coordinates across two neuro-aesthetics meta-analyses (Boccia et al., 2016; Brown et al., 2011). For the reward network mask, the [positive (positive faces + positive objects) > neutral (neutral faces + neutral objects)] contrast was used.

False discovery rate (FDR) for multiple-comparison correction ($p < 0.05$) was used to correct for the number of fROIs in each functional network. One-tailed independent samples *t*-test was used to determine the effects of interest (dynamic > static; bodies > other categories; positive > neutral faces), and FDR multiple-comparison correction ($p < 0.05$) was used to correct for the number of fROIs in each functional network. Furthermore, the percent signal change (PSC) values were extracted from all subject-specific fROIs (MT, EBA, reward network) and then tested in a subsequent Bayesian analysis.

We used the same general Bayesian estimation modelling approach to model PSC. We modelled three perceptual regions in one model and five affective regions in a separate model. We used a Gaussian model rather than ordinal because PSC is a continuous variable. Also, we do not include a varying intercept for item because the ROI data collected from the scanner is averaged across items due to the way trial randomisation works in fast event-related designs.

In terms of priors, we used a weakly informative approach based on our domain knowledge of likely PSC values in fMRI. PSC in fMRI studies are typically small and of the order of 1% for perceptual and cognitive tasks. Therefore, we set the intercept at zero with a normal distribution of 1.5, and we set the population effects and standard deviation priors at zero with a normal distribution of 1. We then constructed four models. Model 1 was an intercepts-only model. Model 2 added stimulus feature motion as a factor. Model 3 added task main effects as a factor. Model 4 added motion * task interactions. Model 4 is displayed below:

```
brm (mvbind (lMT, EBA, rMT) ~ 1 + motion * task.im +
    motion * task.ae +
    (1 + motion * task.im + motion * task.ae | a | pID)
    family = gaussian))
```

3.2.10 | Psychophysiological interaction analysis

The main functional integration hypothesis was that visual seeds (EBA, MT) would interact more with brain circuits associated with reward when rating aesthetics rather than when rating motion or control. To examine this hypothesis, we used psychophysiological interaction (PPI) analysis (Friston et al., 1997). PPI allows the identification of brain areas whose activity correlates with the activity of a seed region as a function of a task (Friston et al., 1997; McLaren et al., 2012). In addition, we used a generalised form of PPI, which enables a wider set of experimental conditions within the main task to be analysed (McLaren et al., 2012). As a consequence, it is possible to see whether any voxels across the brain correlate with the seed region (the ‘physiological’ component) as a function of the two conditions within the main task (the ‘psychological’ component).

The selected seed regions were right EBA, right MT and left MT. These main seed regions were defined based on subject-specific brain coordinates from the univariate fROI analyses. Individual peaks were selected for the seed regions per participant. Despite the fact that we used individual peaks from the univariate analysis to identify the seed regions for the PPI analysis, the analysis is not circular (Kriegeskorte et al., 2009). All regressors from the univariate analysis are taken into account within the PPI model as covariates (O'Reilly et al., 2012). As such, the PPI analyses are statistically independent to the univariate analysis, and thus, the PPI analysis explains additional variance to that which was previously explained by other regressors in the design.

Volumes were generated using a 10-mm sphere, which was positioned on each individual's seed region peak. PPI analyses were run for all seed regions. The PPI model included six regressors from the univariate analyses and the PPI regressors that contained one for each condition of the design (dynamic, static) and one regressor that modelled each seed region activation. To generate the PPI regressors, the time series in the seed regions was defined as the first eigenvariate and was then deconvolved to gauge the underlying neural activity (Gitelman et al., 2003). Subsequently, the deconvolved time series was multiplied by the predicted, pre-convolved time series of each of the two conditions (plus the starter). The resulting PPI for each condition was then convolved with the canonical haemodynamic response function, and the time series of each seed region was included as a covariate (Klapper et al., 2014; McLaren et al., 2012; Spunt & Lieberman, 2012). At the second-level analysis, we investigated the same contrast as in the univariate analyses (dynamic > static). For all group-level

analyses, images were thresholded using a voxel-level threshold of $p < 0.001$ and a voxel-extent (k) of 10 voxels (Lieberman & Cunningham, 2009). We also identify any results that survive correction for multiple comparisons at the cluster level (Friston, 1994) using family-wise error (FWE) correction ($p < 0.05$). In an additional exploratory analysis, we also report whole-brain results for these PPI analyses in order to explore if regions outside of our fROIs were functionally connected to key seed regions.

3.3 | Results

3.3.1 | Behavioural results

The behavioural results replicated Experiment 1 and confirmed that dynamic compared to static stimuli were rated as being more dynamic and aesthetically pleasing (Figure 7; Supplementary Figure S3). These results serve to demonstrate that the stimuli were perceived in a similar manner in a different set of participants and under different conditions (i.e. while within the scanner).

3.4 | fMRI results

3.4.1 | Univariate fROI results

The MT, EBA and reward network fROIs were identified in all participants. The localiser results for each fROI are

reported in Supplementary Table S3. Furthermore, the results for all fROI responses in AE, IM and control tasks compared with baseline, including the regions that survived correction for multiple comparisons, are reported in Supplementary Table S4.

In order to calculate the response profile of fROIs (MT, right EBA, reward network) in AE, IM and control tasks, the PSC values were extracted. PSC values for perceptual and affective fROIs are visualised in Figures 8 and 9 as a function of task and stimulus conditions. In addition, the PSC mean difference scores between dynamic and static stimuli for MT, EBA and affective brain regions are reported in Table 2.

Model comparison was not possible to complete for some analyses of the fROI data, possibly because of the lack of trial-level data. Hence, we turn straight to the interpretation of our key parameter estimates. To do so, we display the parameter estimates across for the most complex model, which is Model 4 (Figure 10a and Table 3). It is not valid statistically to interpret the intercept as being greater than zero because we selected fROIs on the basis that they respond more than zero on average. Therefore, comparisons to zero for the intercept are circular in that they are not independent of the way they were selected. However, the intercept itself is not testing our primary hypothesis, so we can happily ignore it.

In terms of the effect of stimulus feature—implied motion—we can see that the posterior distribution is

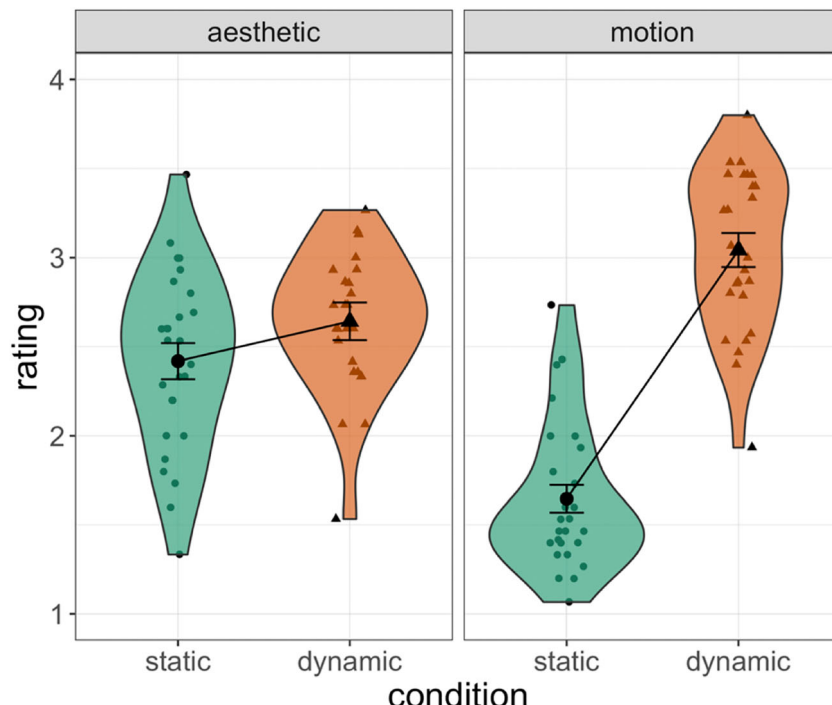


FIGURE 7 Behavioural data from the scanner. Behavioural data collected during scanner illustrate that dynamic stimuli were rated as more aesthetically pleasing and conveying more dynamism than their static counterparts

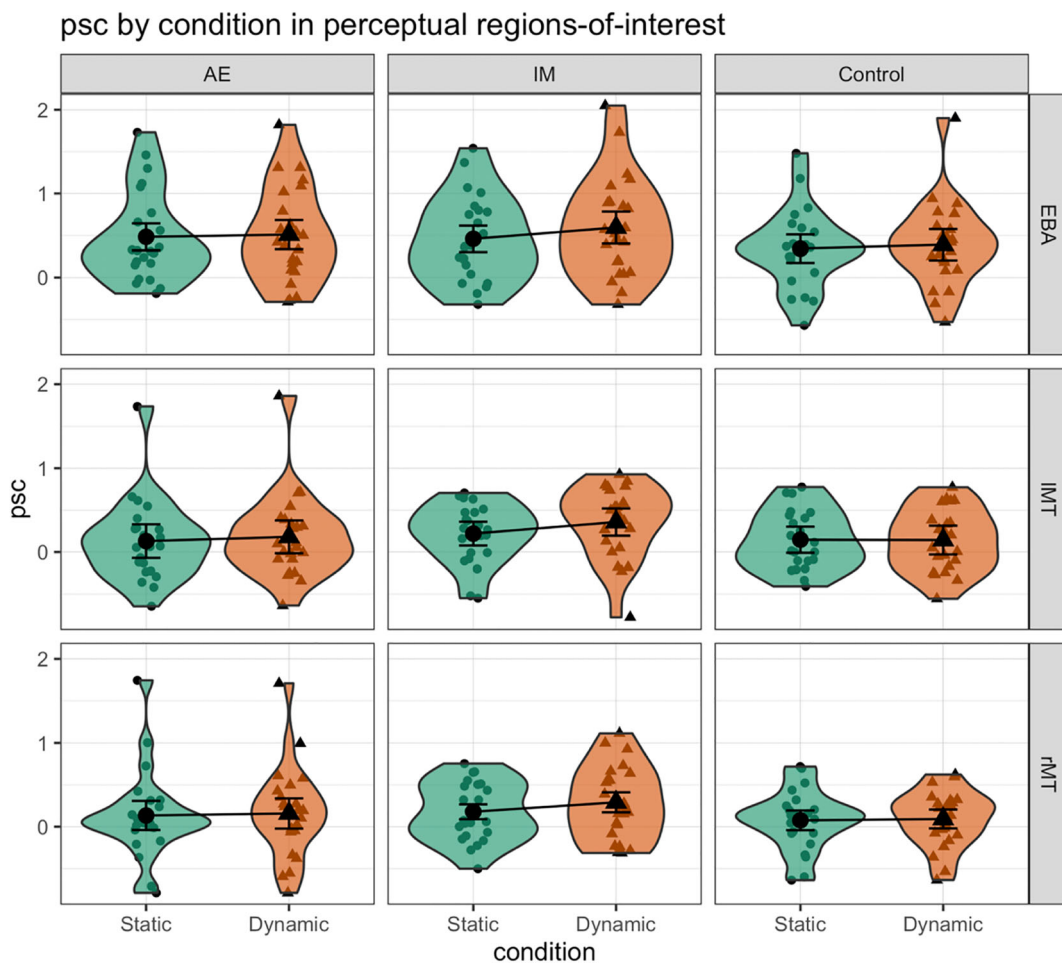


FIGURE 8 Percent signal change (PSC) data from perceptual functional regions of interest (fROIs). Perceptual fROI responses: EBA (extrastrate body area) IMT (left middle temporal area), rMT (right middle temporal area) in aesthetic evaluation task (AE), implied motion task (IM), control. The error bars represent 95% confidence intervals

positive and largely non-overlapping with zero. The same pattern is true for the main effect of motion task with a greater response during the motion task than the other tasks. The aesthetic task main effect was different, however. Only EBA shows a positive response and that remains suggestive. The only interaction effect is that IMT shows a greater response for motion cues in the motion task.

Furthermore, the parameter estimates for affective fROIs are illustrated for the most complex model—Model 4 (Figure 10b and Table 4). The posterior distribution for the effect of stimulus motion overlaps with zero, which suggests invariance to stimulus motion cues in affective regions of interest. In contrast, the posterior distribution for the effect of the implied motion task shows a positive response in bilateral ACC that is non-overlapping with zero. There is also a positive response in left ACC for the aesthetic judgment task that also does not show overlap with zero. No clear non-zero interaction effects were observed.

3.4.2 | Univariate whole-brain analyses

For completeness and for use in future meta-analyses, we also computed group-level whole-brain analyses separately for AE (dynamic > static), IM (dynamic > static) and control (dynamic > static), see Supplementary Table S5. These are also available online at NeuroVault.org (<https://neurovault.org/collections/8542/>).

3.4.3 | Psychophysiological interaction analyses

PSC values for the functional connectivity analyses are displayed in Figure 11. Furthermore, the parameter estimates for the most complex model are displayed in Figure 12. The posterior distribution for the main effects and interactions all overlap with zero. As such, we do not show any clear support for the hypothesis that perceptual ROIs would couple more with affective ROIs as a

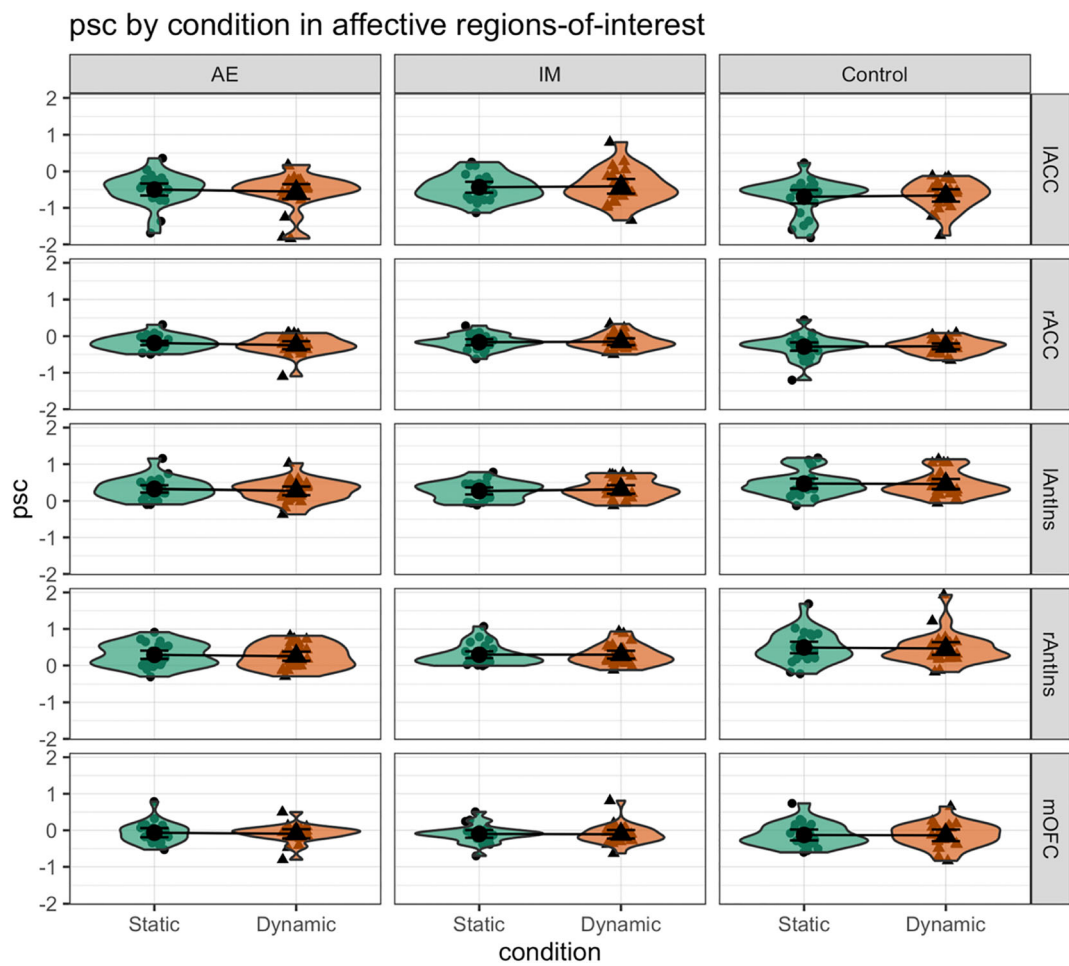


FIGURE 9 Percent signal change (PSC) data from affective functional regions of interest (fROIs). Affective fROI responses—left anterior cingulate cortex (lACC), right anterior cingulate cortex (rACC), left anterior insula (lAntIns), right anterior insula (rAntIns), medial orbitofrontal cortex (mOFC)—in aesthetic evaluation task (AE), implied motion task (IM), control. The error bars represent 95% confidence intervals

function of the stimulus features (dynamic versus static, as reflected by the intercept) or the type of task (aesthetic or motion tasks compared to the control task, as reflected by task or region*task interactions).

Furthermore, we report the results from exploratory PPI whole-brain analyses, aimed to identify whether regions outside of our fROIs were functionally coupled to perceptual key seed regions as a function of experimental tasks (Figure 13). Figure 13a shows that while making an aesthetic judgement, EBA was functionally coupled to several brain regions, such as the superior parietal lobule and the paracentral lobule (clusters in green), whereas left MT demonstrated functional coupling to the right calcarine gyrus (shown in magenta). In addition, Figure 13b shows that while evaluating the level of the perceived dynamism, both right and left MT were functionally coupled to several brain regions, such as the fusiform gyrus (clusters in green) and the

middle occipital gyrus (clusters in red). For a complete set of PPI whole-brain analyses results, see Supplementary Tables S7–S9. We also provide the whole-brain PPI t-maps at NeuroVault.org (<https://neurovault.org/collections/8542/>).

4 | GENERAL DISCUSSION

Current understanding of how the brain constructs aesthetic experiences is in its infancy, and the mapping between brain structure and function remains relatively coarse. Here, we provide the most comprehensive evidence to date regarding the functional contribution of visual and affective information processing units to the aesthetic evaluation of visual artworks with implied motion cues. Our results do not support our primary hypotheses regarding integration between neural systems

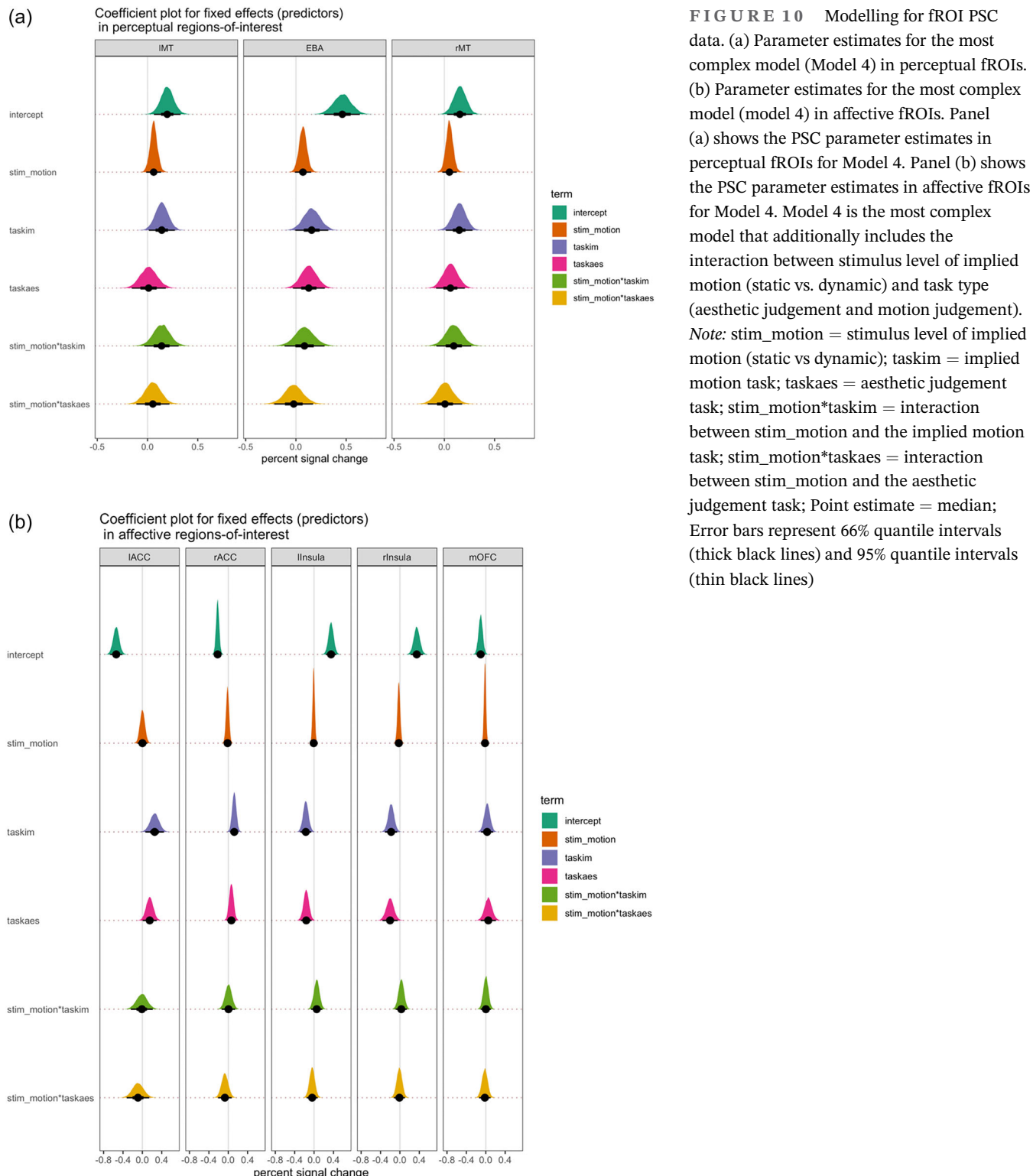
TABLE 2 Percentage signal change mean difference scores between dynamic and static stimuli on AE, IM and control for right EBA, MT and reward brain circuit regions

fROIs	Task	Mean Difference		Cohen's <i>d</i>
		Dynamic > static	[95% CI]	
Right EBA	AE	0.03	[−0.13, 0.18]	0.11
	IM	0.13	[−0.02, 0.29]	0.55
	Control	0.05	[−0.11, 0.20]	0.19
Right MT	AE	0.02	[−0.12, 0.16]	0.12
	IM	0.11	[−0.03, 0.25]	0.52
	Control	0.02	[−0.12, 0.16]	0.07
Left MT	AE	0.05	[−0.09, 0.19]	0.23
	IM	0.14	[−0.01, 0.28]	0.63
	Control	−0.01	[−0.15, 0.14]	−0.02
Left ant. insula	AE	−0.05	[−0.17, 0.06]	−0.30
	IM	0.04	[−0.07, 0.16]	0.23
	Control	−0.01	[−0.13, 0.10]	−0.08
Right ant. insula	AE	−0.04	[−0.17, 0.09]	−0.20
	IM	−0.01	[−0.13, 0.13]	−0.01
	Control	−0.03	[−0.16, 0.10]	−0.15
Medial OFC	AE	−0.03	[−0.14, 0.08]	−0.18
	IM	−0.01	[−0.12, 0.10]	−0.05
	Control	−0.01	[−0.12, 0.10]	−0.06
Right ACC	AE	−0.06	[−0.20, 0.08]	−0.28
	IM	0.01	[−0.12, 0.15]	0.06
	Control	0.01	[−0.13, 0.15]	0.04
Left ACC	AE	−0.06	[−0.28, 0.17]	−0.16
	IM	−0.06	[−0.42, 0.29]	−0.11
	Control	0.05	[−0.19, 0.26]	0.10

Abbreviations: AE, aesthetic evaluation; CI, confidence interval; IM, implied motion; left ACC, left anterior cingulate cortex; medial OFC, medial orbitofrontal cortex; right ACC, right anterior cingulate cortex.

associated with body perception, motion and affective processing during the aesthetic appreciation of dynamic paintings. Therefore, we cannot confidently state that EBA, MT and brain systems associated with reward processing play a unique functional role in the computation of aesthetic evaluation of paintings with implied motion. Instead, we show suggestive evidence that motion and body-selective systems may integrate signals via functional connections with a third neural network in dorsal parietal cortex, which may act as a relay or integration site. Overall, our findings clarify the roles of several neural circuits in the way that motion cues give rise to aesthetic preferences while also setting up a range of future directions to pursue that involve further exploration of how neural networks exchange signals during aesthetic judgements.

Three prior studies have investigated visual motion processing unit MT in relation to aesthetic evaluations, and they have produced mixed findings (Di Dio et al., 2016; Kim & Blake, 2007; Thakral et al., 2012). We confirm the pattern of results found by Thakral et al. (2012)—namely, that MT is sensitive to implied motion cues in paintings while being insensitive to aesthetic judgements based on those cues. That is, MT responds to stimulus features that imply motion and tasks that involve motion judgements. However, MT shows no sensitivity to tasks that involve aesthetic judgements. Compared with prior studies, therefore, our findings emphasise the value of using a fROI approach and testing larger sample sizes. Indeed, prior work that implicated MT in aesthetic judgements either did not functionally localise MT (Di Dio et al., 2016) or



used small sample sizes (e.g. $N = 5$ in a key analysis; Kim & Blake, 2007), which makes firm functional conclusions difficult. One notable difference to Kim and Blake's (2007) study concerns expertise. Kim and Blake (2007) only showed sensitivity to aesthetic judgements of implied motion in those individuals with art

experience. Therefore, it is possible that MT is insensitive to aesthetic judgements in those with minimal exposure to art but becomes increasingly sensitive as experience with art develops. Future research that explores further how prior experience shapes the neurobiology of aesthetic preferences would be welcomed, as

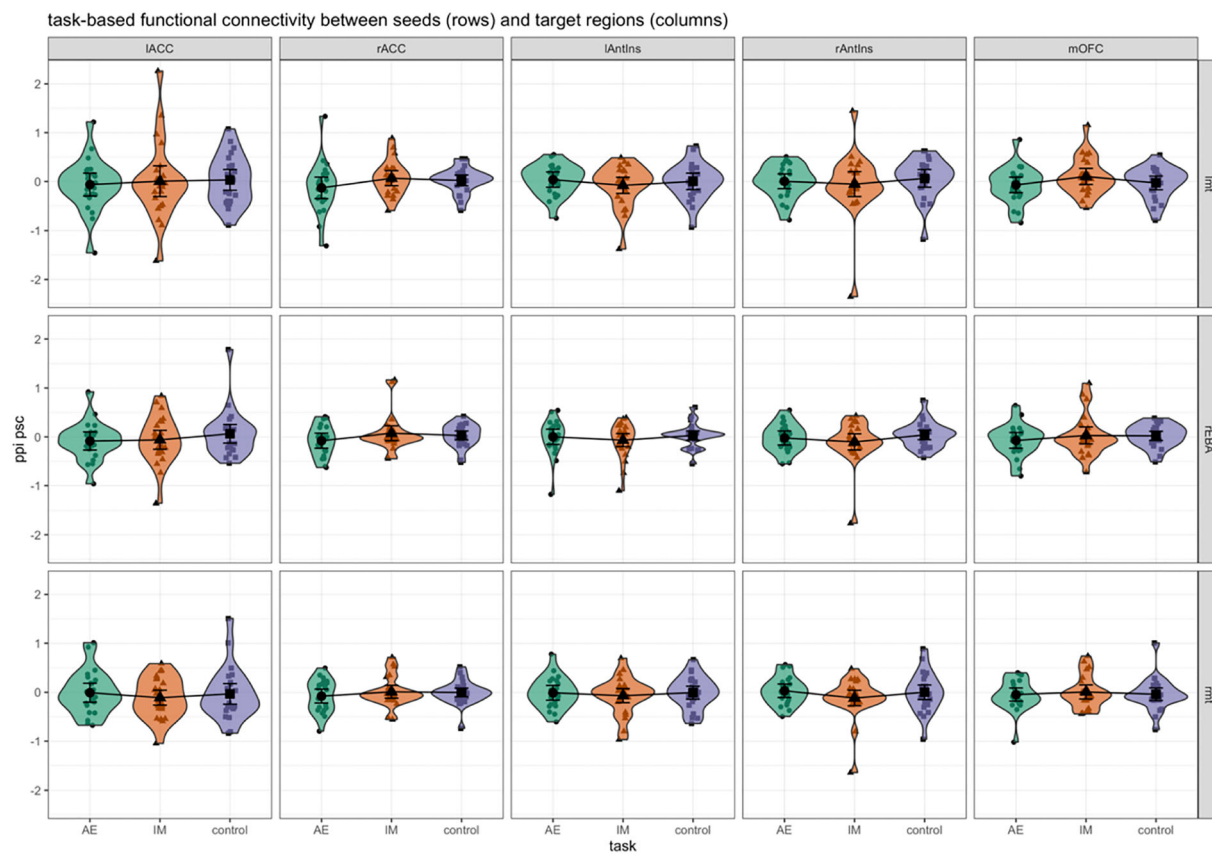


FIGURE 11 Percent signal change (PSC) in functional connectivity analyses. This figure illustrates the PSC in functional integration between the perceptual seed regions (rows) and the affective target regions (columns) as a function of the main experimental tasks (aesthetic judgement, motion judgement and control). *Note:* Perceptual seed regions—lMT, left middle temporal area; rEBA, right extrastriate body area; rMT, right middle temporal area; affective target regions—lACC, left anterior cingulate cortex; rACC, right anterior cingulate cortex; lAntIns, left anterior insula; rAntIns, right anterior insula; mOFC, medial orbitofrontal cortex—in aesthetic evaluation task (AE), implied motion task (IM) and control. The error bars represent 95% confidence intervals

ACC has been implicated in aesthetic judgements specifically previously (Brown et al., 2011; Ishizu & Zeki, 2011, 2017; Vartanian & Goel, 2004), here we show a more general task effect when making aesthetic and non-aesthetic judgements about paintings in general, which is consistent with the well-documented role that the ACC plays in a range of different tasks that are associated with the multiple-demand network (Crittenden et al., 2016; Duncan, 2010; Kolling et al., 2016). One unexpected result was that the bilateral anterior insula was engaged more in the control task rather than in aesthetic evaluation task. We speculate that this response may reflect the different attentional demands that the control task required compared with the aesthetic task (Simmons et al., 2011). Furthermore, our results did not show sensitivity to aesthetic judgements in mOFC, even though previous research has linked mOFC engagement to processing artistic beauty (Ishizu et al., 2014; Kawabata & Zeki, 2004; Zhang et al., 2017). We speculate this lack of response in mOFC might be due to the homogeneity of the stimuli used, which were all portraits of a

particular kind, rather than a more varied stimulus set. However, as our findings are in consensus with other research studies (Di Dio et al., 2016; Silveira et al., 2015; Thakral et al., 2012), we hope that mOFC's involvement in aesthetic appreciation of paintings with implied motion might be clarified by future research.

Although we had key hypotheses regarding functional connectivity between nodes in the ventral visual stream and nodes in the affective network, we showed no support for such relationships. However, given that prior work has shown that perceptual and affective nodes are functionally coupled when people express their musical aesthetic preference (Sachs et al., 2016), we acknowledge that this lack of coupling may reflect a false negative. For example, it is possible that the effects were smaller than we could detect with confidence or that a different analytical approach may be required to reveal them. In contrast, our whole-brain approach did offer suggestive evidence for coupling between EBA and superior parietal regions as a function of aesthetic evaluation task. Such findings may implicate a possible link between

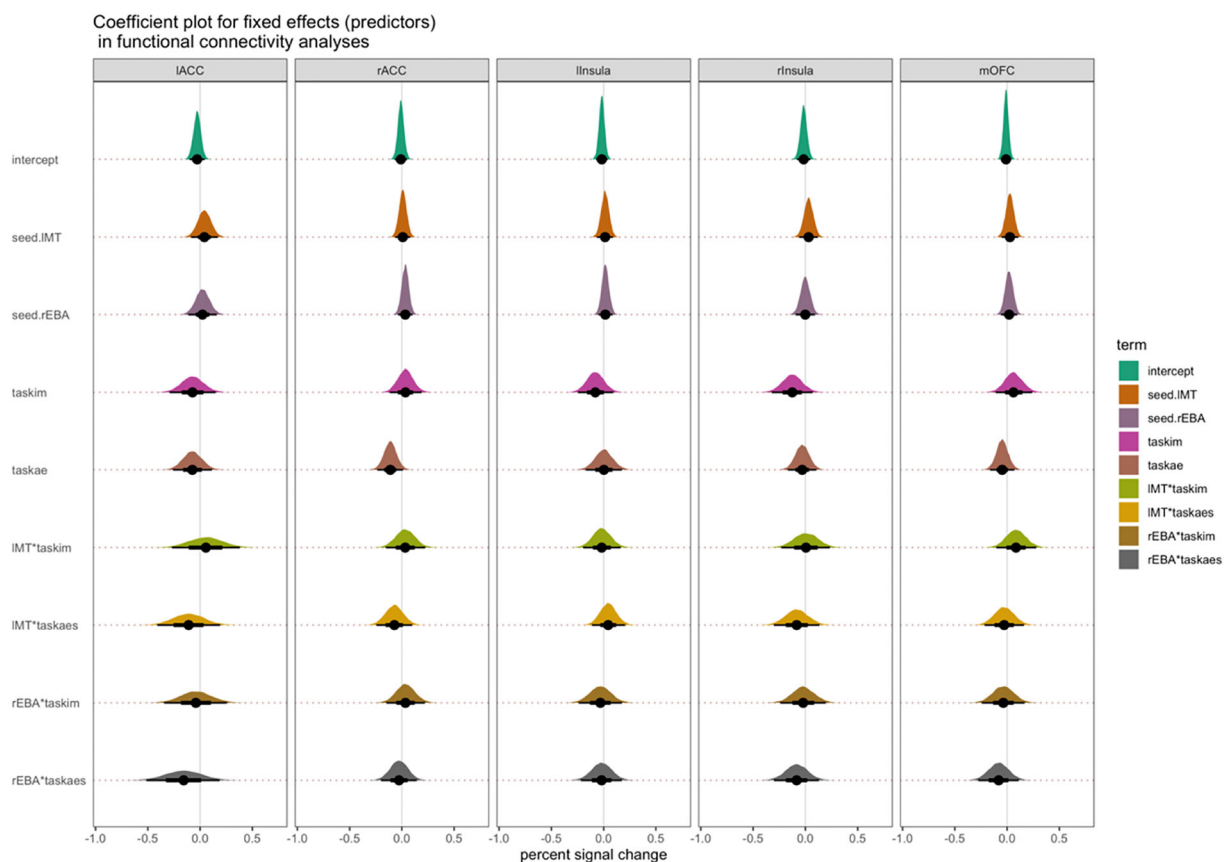
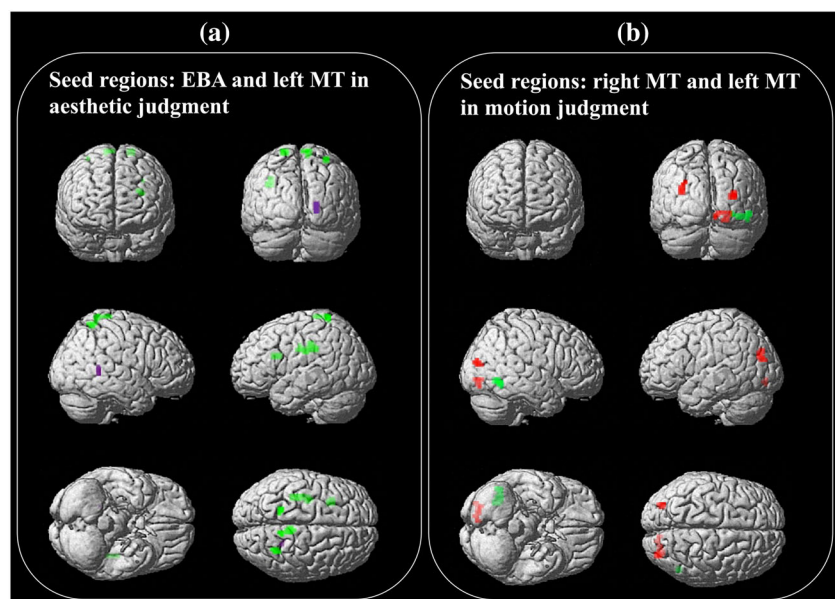


FIGURE 12 Modelling results from the functional connectivity analyses. This figure illustrates the PSC parameter estimates from the functional connectivity analyses. The columns represent the affective target regions, whereas the rows indicate the key models. Note: Labels for affective target regions are as in Figure 11; seed.lMT, seed region left MT; seed.rEBA, seed region right EBA; taskim, implied motion task; taskaes, aesthetic judgement task; IMT*taskim, interaction between left MT and implied motion task; IMT*taskaes, interaction between left MT and aesthetic judgement task; rEBA*taskim, interaction between right EBA and implied motion task; rEBA*taskaes, interaction between right EBA and aesthetic judgement task; Point estimate = median; Error bars represent 66% quantile intervals (thick black lines) and 95% quantile intervals (thin black lines)

FIGURE 13 Results from the PsychoPhysiological interaction (PPI) whole-brain analyses. Panel (a) illustrates the functional coupling of EBA to superior parietal regions (green) and left MT to right calcarine gyrus (magenta) in aesthetic judgement task. Panel (b) shows the functional coupling of right MT and left MT to middle occipital regions (red and green) in implied motion judgement task. Voxel-wise threshold used for images was $p < 0.001$, $k = 10$. Note: Labels for seed regions are similar to Figure 12



endowed beauty: An fMRI study. *Scientific Reports*, 7(1), 7125. <https://doi.org/10.1038/s41598-017-07608-8>

Zimmermann, M., Mars, R. B., de Lange, F. P., Toni, I., & Verhagen, L. (2018). Is the extrastriate body area part of the dorsal visuomotor stream? *Brain Structure and Function*, 223(1), 31–46. <https://doi.org/10.1007/s00429-017-1469-0>

SUPPORTING INFORMATION

Additional supporting information may be found in the online version of the article at the publisher's website.

How to cite this article: Bara, I., Darda, K. M., Kurz, A. S., & Ramsey, R. (2021). Functional specificity and neural integration in the aesthetic appreciation of artworks with implied motion. *European Journal of Neuroscience*, 1–29. <https://doi.org/10.1111/ejn.15479>